Appendix

Hepatic stellate cells limit hepatocellular carcinoma progression through the orphan receptor endosialin

Carolin Mogler,[1,2,3]*, Courtney König[1,4]*, Matthias Wieland[1,4], Anja Runge[1,4], Eva Besemfelder[1], Dorde Komljenovic[5], Thomas Longerich[6], Peter Schirmacher[2], and Hellmut G. Augustin[1,4,7]

[1]Division of Vascular Oncology and Metastasis, German Cancer Research Center Heidelberg (DKFZ-ZMBH Alliance), Germany; [2]Institute of Pathology, Heidelberg University, Germany; [3]Institute of Pathology, Technical University Munich, Germany; [4]Department of Vascular Biology and Tumor Angiogenesis (CBTM), Medical Faculty Mannheim, Heidelberg University, Germany; [5]Department of Medical Physics in Radiology, German Cancer Research Center Heidelberg, Germany; [6]Institute of Pathology, RWTH Aachen, Germany; [7]German Cancer Consortium, Heidelberg Germany.

Table of contents

Appendix Figure S1

Appendix Figure S1. Endosialin expression on human dysplastic nodules (whole tissue slides). Immunohistochemical staining for Endosialin on whole tissues slides of Dysplastic nodules (200x magnification). Scale bar: as indicated.

Appendix Figure S2
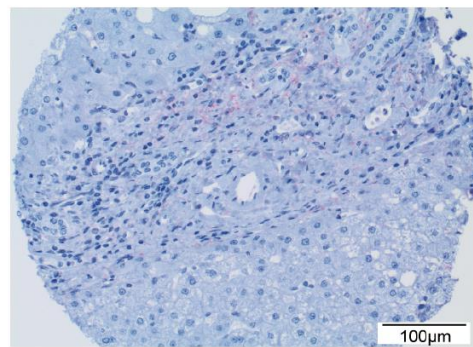
Peritumorous liver
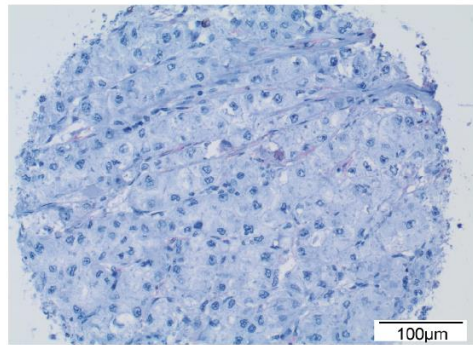
HCC
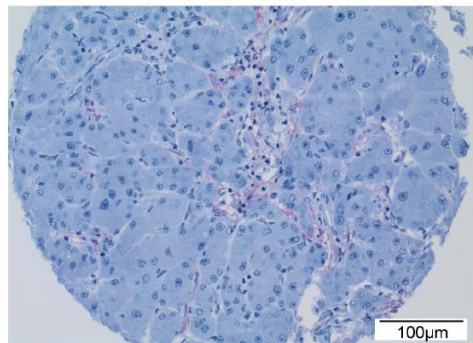
HCC

Appendix Figure S2. Heterogeneous Endosialin expression on HCC tissue microarray punches. Immunohistochemical stainings of Endosialin on 57 HCC and peritumorous liver parenchyma tissue microarray punches. Scale bars: as indicated. HCC=hepato-cellular carcinoma.

Appendix Figure S3
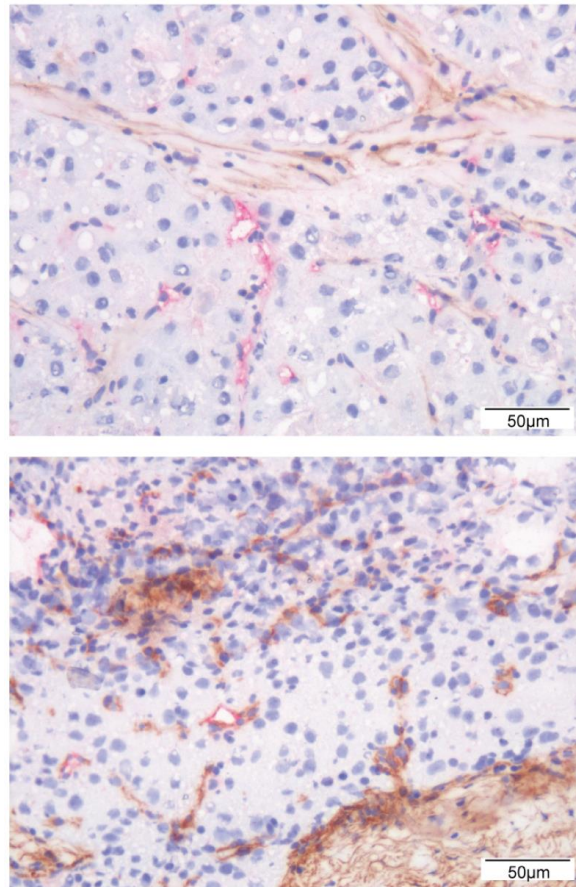
Appendix Figure S3. Co-stainings of Endosialin and CD31 on human HCC. Immunohisto-chemical double staining of Endosialin (brown) and CD31 (red) of different HCC samples (n=8). Scale bars: as indicated.
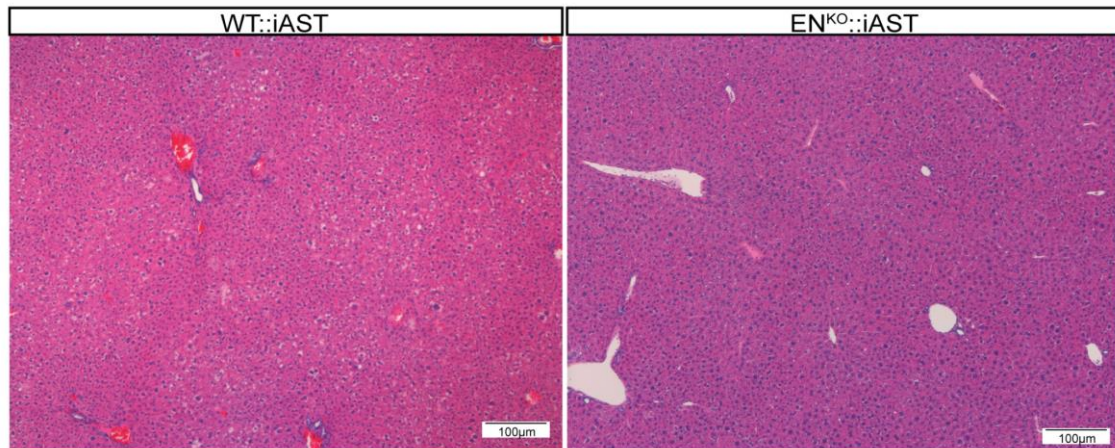
Appendix Figure S4

Appendix Figure S4. Immunohistochemical analysis of non-tumorigenic WT and Endosialin-deficient livers. HE stainings of WT::iAST and EN^{KO}::iAST livers in un-challenged settings do not display any overt phenotype. Scale bars: as indicated.
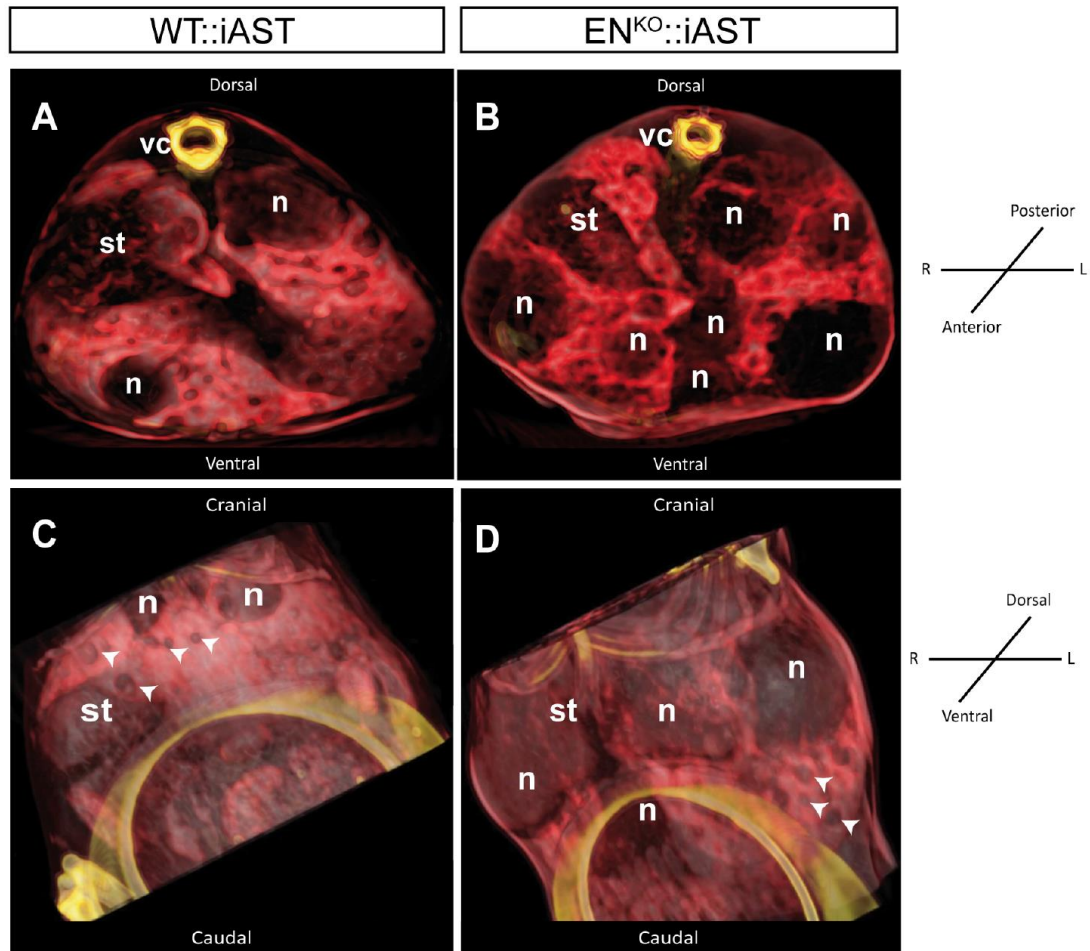
Appendix Figure S5

Appendix Figure S5. Computer tomographical analysis of tumorigenic WT and Endosialin-deficient mice. Computer tomography of WT::iAST (A, C,) and EN^KO::iAST (B,D) mice seven weeks after tumor induction as described in Figure 2. 2-dimensionally and 3-dimensionally reconstructed images. n= nodule; st=stomach; vc= vertebral cord.

Appendix Figure S6
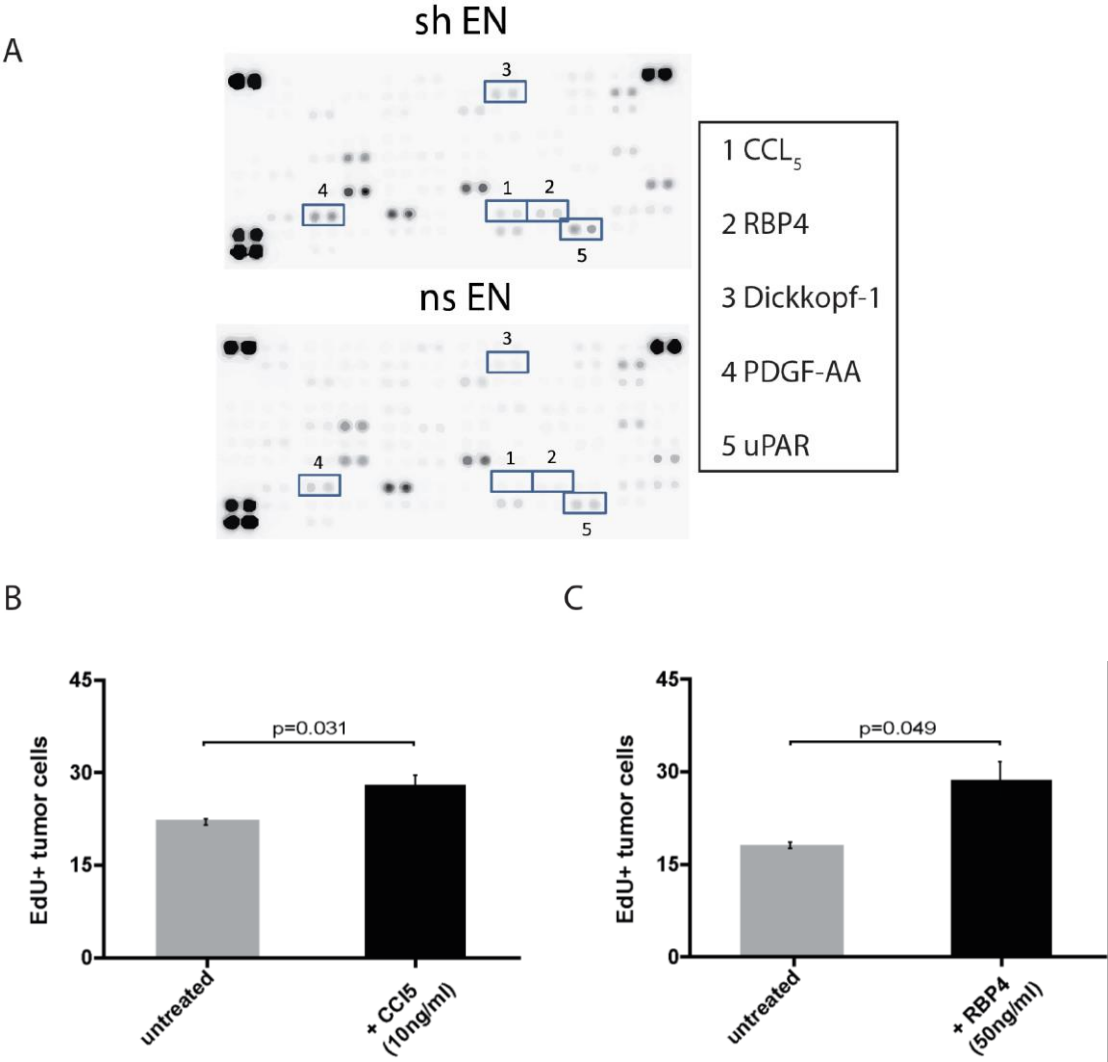
Appendix Figure S6. Expression profiling and functional analysis of conditioned media from nsEN and shEN HSC. Cytokine array of CM from nsEN and shEN HSC highlighting the top 5 differentially expressed cytokines (A). EdU proliferation assay of Huh7 tumor cells stimulated with the top 2 cytokine candidates: CCl5 (B) or RBP4 (C). n=1 with 3 technical replicates. Data are expressed as mean ± SD. Statistical analysis: Student´s t-test.

Appendix Table S1.

List of cytokines. Human cytokine array from the conditioned media of shEN and nsEN HSC.

Cytokine	nsEN	shEN	shEN/nsEN	Cytokine	nsEN	shEN	shEN/nsEN
RANTES/CCL5	2.32	14.63	6.31	EGF	7.47	5.89	0.79
RBP4	3.57	18.31	5.13	CRP	5.22	4.08	0.78
DKK-1	6.60	21.04	3.19	BDNF	4.69	3.66	0.78
PDGF-AA	22.49	59.18	2.63	Ang-1	2.66	2.04	0.77
uPAR	22.50	54.57	2.43	IL-17A	24.04	18.02	0.75
CCL2/MCAF/MCP-1	58.57	132.86	2.27	IL-3	1.97	1.46	0.74
Flt-3 Ligand	1.06	2.17	2.05	FGF basic/FGF-2	7.44	5.49	0.74
IL-1 R4/ST2L	1.90	3.60	1.89	IL-11	7.10	5.21	0.73
Cripto-1	1.36	2.49	1.83	Complement Factor D	4.12	2.98	0.72
Osteopontin (OPN)	7.19	12.74	1.77	IL-18 Bpa	1.58	1.14	0.72
Complement Component C5/C5a	0.93	1.48	1.59	CXCL5	2.96	2.11	0.71
DPPIV/CD26/DPP4	0.59	0.94	1.59	IL-16	1.51	1.07	0.71
TGFA	0.34	0.52	1.51	IL-6	9.28	6.51	0.70
FGF-7	0.81	1.21	1.49	Angiogenin	1.51	1.04	0.69
IGFBP-2	1.06	1.55	1.46	IL-27	4.32	2.96	0.68
MMP-9	42.84	58.20	1.36	IL-1b	4.13	2.81	0.68
Endoglin/CD105	8.89	11.03	1.24	Vitamin D BP	6.21	4.12	0.66
Thrombospondin-1/TSP-1	17.63	21.86	1.24	CXCL9/MIG	2.96	1.95	0.66
Relaxin-2/RLN2/RLXH2	2.62	3.16	1.21	IL-19	4.27	2.64	0.62
MIF	99.51	118.73	1.19	Ang-2	8.08	4.97	0.61
CD14	6.68	7.68	1.15	IL-24	5.26	3.23	0.61
LIF	1.42	1.54	1.09	IL-1a	6.12	3.71	0.61
EMMPRIN	42.89	46.29	1.08	IL-22	7.25	4.39	0.61
Cxcl4/PF4	2.15	2.31	1.08	IL-32a/b/g	3.02	1.82	0.60
SHBG/ABP	5.36	5.66	1.06	Adiponectin	5.89	3.54	0.60
TFF3/ITF	5.63	5.94	1.05	ICAM-1/CD54	3.36	2.01	0.60
CCL7/MCP-3/MARC	1.31	1.37	1.05	IL-12 p40	2.97	1.76	0.59
GDF-15/MIC-1	3.11	3.25	1.04	TNFa	1.76	1.03	0.58
CD71/TfR	3.15	3.21	1.02	CCL17/TARC	3.11	1.79	0.58
G-CSF	0.66	0.68	1.02	IL-1ra	2.09	1.15	0.55
Cystatin C	2.40	2.39	0.99	IFN-g	5.88	3.21	0.55
CD30/TNFRSF8	4.64	4.60	0.99	Lipocalin-2	5.24	2.84	0.54
IL-13	1.23	1.18	0.96	BAFF/BLyS/TNFSF13B	2.74	1.48	0.54
CXCL11/I-TAC	0.71	0.68	0.96	Kallikrein 3/PSA/KLK3	5.19	2.75	0.53
Serpin E1	239.90	231.04	0.96	IL-33	2.02	1.04	0.51
IL-15	249.04	239.28	0.95	CD40 ligand/CD40L/TNFSF5/CD154/TRAP	7.67	3.93	0.51
CXCL10/IP-10	3.41	3.23	0.94	IL-4	2.01	1.01	0.50
IGFBP-3	3.49	3.29	0.94	Fas Ligand	2.82	1.37	0.49
CCL3/CCL4/MIP-1a/b	1.03	0.96	-0.36	IL-2	2.01	0.96	0.48
IL-10	2.55	2.34	0.92	IL-5	1.89	0.81	0.43
FGF-19	16.08	14.76	0.92	RAGE	1.03	0.41	0.40
GM-CSF	13.59	12.06	0.89	Myeloperoxidase	3.28	1.19	0.36
PDGF-AB/BB	1.16	1.03	0.88	CCL20/MIP-3a	0.94	0.31	0.33
Pentraxin-3/PTX3/TSG-14	128.18	112.91	0.88	Chitinase 3-like 1	2.49	0.80	0.32
CSF-1/M-CSF	5.49	4.81	0.88	Aggrecan 1	2.73	0.84	0.31
Cxcl12/SDF-1a/PBSF	12.79	11.16	0.87	CXCL1/GRO-a	2.44	0.72	0.29
Resistin	9.56	8.32	0.87	Leptin/OB	3.06	0.88	0.29
VEGF	4.16	3.61	0.87	Growth hormone	1.95	0.44	0.23
IL-8	71.49	61.13	0.86	HGF	2.63	0.58	0.22
IL-31	2.19	1.86	0.85	CCL19/MIP-3b	0.64	0.09	0.14
IL-23	1.06	0.89	0.84				
IL-34	0.51	0.41	0.81				